

# Comparative analysis of the performance of a dual-fuel internal combustion engine for CNG and gasoline fuels

Mohammad Ameri<sup>\*,a</sup>, Farzad Kiaahmadi<sup>a</sup>, Mansour Khanaki<sup>b</sup>

<sup>a</sup>*Department of Mechanical & Energy Engineering, Power & Water University of Technology  
East Vafadar Blvd., Tehranpars, Tehran, Iran*

<sup>b</sup>*Department of Mechanical Engineering, Imam Khomeini International University  
Qazvin, Iran*

## Abstract

In this paper, the performance of a dual-fuel internal combustion engine for CNG and gasoline fuels is evaluated at the steady-state condition through energy and exergy analysis using experimental test results. The energy and exergy balances are calculated at different engine speeds. The results show that the energy and exergy of the heat rejection for gasoline and CNG fuels increases with increasing engine speed and the exergy efficiencies are slightly higher than the corresponding energy efficiencies. Moreover, the results show that the exergy efficiency for CNG-fuel is higher than the gasoline-fuel exergy efficiency at all engine speeds. The results show that due to volumetric efficiency drop, the power and torque of the CNG-fuel engine are lower than for the gasoline-fuel engine. Furthermore, the specific fuel consumption of the CNG-fuel engine is lower than for the gasoline-fuel one. The results of this study demonstrate that the key source of system inefficiency is the destruction of exergy by irreversible processes, mostly combustion. Moreover, it should be noted that liquid fuels like gasoline have many important advantages like much greater volumetric energy density, ease of transport and storage, which have made them the preferred fuels for IC engines.

**Keywords:** Dual-fuel engine, Exergy analysis, Efficiency, Irreversibility, Performance

## 1. Introduction

Exergy analysis is a significant tool for assessing energy systems [1]. In recent years, many engineers and scientists have suggested that the thermodynamic performance of a process is best evaluated by performing an exergy analysis in addition to or in place of the conventional energy analysis, because the exergy analysis appears to provide more insights and is more useful in efficiency improve-

ment efforts than an energy analysis on its own [2]. Many researchers have studied exergy analysis, also known as second law or availability analysis, of internal combustion engines. Alasfour [3] performed an exergy analysis of an SI engine to assess the application of a butanol-gasoline blend fuel. Alkidas [4] performed an energy and exergy analysis of a diesel engine using experimental data. Lipkea and DeJooede [5] studied the comparative energetic and exergetic performances of two direct injection diesel engines. Caton [6] reviewed many previous studies on the exergetic performance of internal combustion engines. Rakopoulos and Giakoumis recently presented second law analyses applied to internal com-

\*Corresponding author

Email addresses: ameri\_m@yahoo.com (Mohammad Ameri<sup>\*</sup>), kiaahmadifarzad2005@yahoo.com (Farzad Kiaahmadi), khanaki.m@gmail.com (Mansour Khanaki)

bustion engines operation [7]. Caton [8] presented an analysis on the destruction of availability (exergy) owing to combustion processes with specific application to internal combustion engines. Kopac and Korkturk [9] determined the optimum speed of an internal combustion engine by exergy analysis. Rakopoulos and Kyritsis [10] presented a comparative second law analysis of internal combustion engine operation for methane, methanol, and dodecane fuels. Sayin et al. [11] presented comparative energy and exergy analyses of a four-cylinder, four-stroke spark-ignition engine using gasoline fuels of three different research octane numbers (RONs). Nakonieczny [12] presented entropy generation in a diesel engine turbocharging system. Rakopoulos and Giakoumis [13] presented an availability analysis of a turbocharged diesel engine operating under transient load conditions. Canakci and Hosoz presented energy and exergy analyses of a diesel engine fuelled with various biodiesels [14]. Ameri et al. [15] studied energy and exergy analyses of a spark-ignition engine. They found the optimum engine speed and concluded that determination of the optimum engine speed should not be based merely on an energy analysis alone.

The objective of this study is to evaluate and to compare the performance of a dual-fuel engine at the steady state condition through energy and exergy analysis by using the experimental test results as well as to determine the optimum speed of a dual-fuel engine using combined energy and exergy analysis. Using the steady state test results consisting of flow rate, temperature, pressure, power, torque, and the reaction equations, the energy and exergy rate balances for the dual-fuel engine were determined. Moreover, the performance parameters of the engine for each fuel, namely the fuel energy, specific fuel consumption, heat rejection by the cooling water, heat rejection by the exhaust gas, miscellaneous heat rejection, energy efficiency, exhaust exergy, heat exergy, work exergy, fuel exergy, exergy efficiency, and exergy destroyed in the engine, were computed and compared with each other. The tests were conducted in an industrial-scale facility of the Iran Khodro Powertrain Company (IPCO), which is equipped with advanced, state-of-the-art test instruments. It enabled the authors to follow the real conditions of engine operation at different speeds.

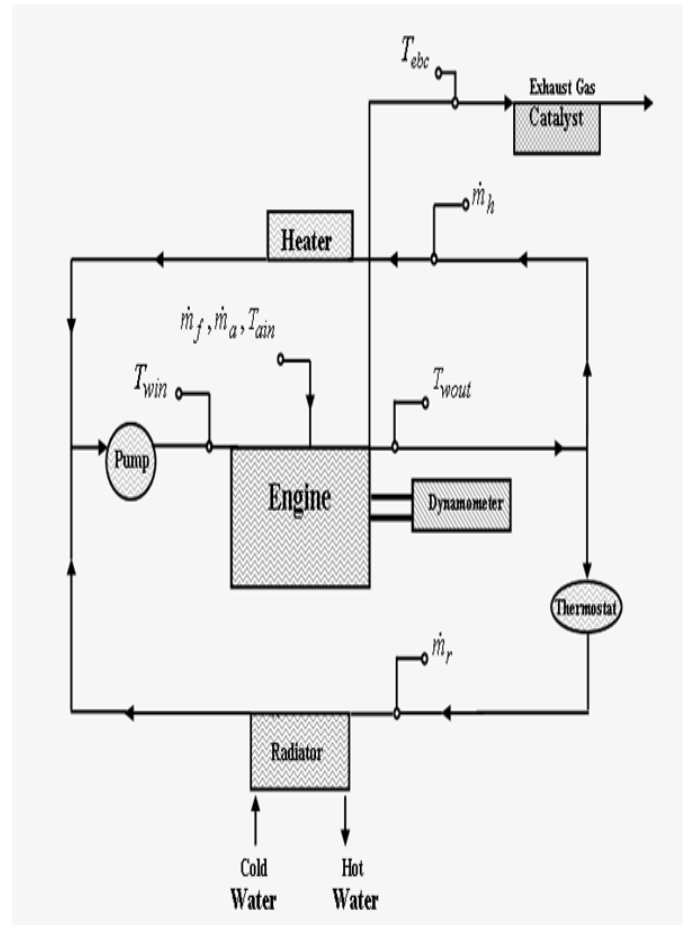


Figure 1: Schematic of engine test unit

## 2. Experimental study

The tests were performed on a four-cylinder, four-stroke Iran Khodro XU7 JPL3 1.8 L spark ignition engine, which originally requires 95-RON gasoline. The schematic of the test unit is shown in Figure 1 and details of the engine specifications are shown in Table 1.

The fuels used in the test engine are: commercial-grade gasoline of 95-RON with the typical formula and CNG. The fuel compositions of CNG are given in Table 2.

The experiments were conducted on an existing test unit at IPCO. The experimental set-up enabled the authors to make accurate measurements of fuel, air and water flow rates, engine load, speed and torque, the inlet and outlet coolant temperature and the temperature of air and exhaust gas.

The water mass flow rates in the radiator, heater and engine were measured. The test was carried

Table 1: The technical specifications of the Iran Khodro XU7 JPL3 engine

Engine type	XU7 JPL3
Cylinder number	4
Cylinder bore	83 mm
Stroke	81.4 mm
Firing order	1,342
Static ignition timing, °	30.1 BTDC at 4,200 rpm manifold air pressure 80 kPa
Static ignition timing, °	26 BTDC at 4,200 rpm manifold air pressure 90 kPa
Intake valve opens, °	81 BTDC
Intake valve 1mm lift	61 BTDC
Intake valve maximum lift (9.7 mm)	94 ATDC
Total cylinder volume	1,761 cm <sup>3</sup>
Compression ratio	9.25:1
Maximum torque	152.75 Nm at 2,500 rpm
Maximum power	68.65 kW
Engine octane requirement	95 RON

Table 2: Fuel compositions of CNG

Fuel composition	Percent, %
CH <sub>4</sub>	88.1
C <sub>2</sub> H <sub>6</sub>	4.7
C <sub>3</sub> H <sub>8</sub>	1.02
C <sub>4</sub> H <sub>10</sub>	0.47
C <sub>5</sub> H <sub>12</sub>	0.17
C <sub>6</sub> H <sub>14</sub>	0.04
CO <sub>2</sub>	1
N <sub>2</sub>	4.5

Table 5: The accuracies of the measurements and the uncertainties in the calculated results

Measurements	Accuracy
Load	±2 N
Speed	±25 rpm
Time	±0.5%
Temperatures	±1°C
Calculated results	Uncertainty
Power	±2.55%
SFC	±2.60%

out on a fired test bench. The coolant system is a pressurized system with pressure of 1.4–1.8 bar. For the natural aspirated engine, the original radiator was installed in a water reservoir for the heat emission. A heater was mounted as well. The engine was equipped with the required measurement devices.

Table 3 shows the type and the temperature range of the sensors. The sensors were calibrated before any test. The coolant temperature was measured at the engine inlet, engine outlet, radiator inlet, radiator outlet, heater inlet and heater outlet positions. The coolant flow was measured by a flow meter with accuracy of 0.01 m<sup>3</sup>/h. It registered the complete coolant flow at the water pump inlet and heater flow at inlet or outlet positions as well as radiator flow at

inlet or outlet locations.

The fuel supply mode for both gasoline and CNG is multi-injection.

The engine was operated at full load. The engine speed variation was done from a speed of 1000 rpm to a maximum speed of 6000 rpm in 500 rpm steps. The coolant inlet temperature was set at . The input air pressure of the engine is equal to 101.325 kPa using an air-conditioning system (at sea level). The coolant characteristic values at the nominal coolant inlet temperatures of are shown in Table 4.

The accuracies of the measurements and the uncertainties in the calculated results are given in Table 5. The experimental results for different engine speeds from 1,500 to 6,000 rpm are summarized in Tables 6 and 7.

Table 3: The technical specifications of the sensors

Designation	Sensor Type	Range	Accuracy	Producer
Measuring coolant temperature	PT 100	0–200°C	0.1% Full scale	Druck
Measuring exhaust gas temperature	K	0–200°C	0.1% Full scale	Enderss & Hauser
Measuring pressure	Piezoelectric & Piezoresistive	0–10 kPa	0.12% Full scale	Jumbo

Table 4: Coolant characteristic values for the nominal coolant inlet temperatures (90°C)

Values	Coolant pressure upstream pump(absolute) (bar)	Water (bar)	$\Delta T_{coolant}$ (stationary)	Engine rated speed, °C	Oil temperature main gallery, °C
Min. value		>1		-	-
Target. value		1.5		8	140
Max. value		1.8		10	150

Coolant content: 50% water and 50% glycol.

Table 6: Experimental test results for the engine at different speeds in gasoline mode

$n_{es}$ , rpm	$\tau_{et}$ , Nm	$N_e$ , kW	$\dot{m}_f$ , kg/h	$\dot{m}_a$ , kg/s	$\dot{m}_r + \dot{m}_h$ , Lit/min	$\lambda$	$T_{amb}$ , °C	$T_{ain}$ , °C	$T_{win}$ , °C	$T_{wout}$ , °C	$T_{ebc}$ , K
1500	127.78	20.03	5.98	0.023	43.48	0.97	31.21	27.77	85.54	90.56	844.32
2000	132.07	27.57	8.66	0.030	58.11	0.85	31.90	27.48	85.25	89.81	869.52
2500	152.75	39.93	11.12	0.042	72.75	0.92	32.06	27.89	85.21	90.33	980.92
3000	146.98	46.07	13.15	0.049	87.61	0.90	37.54	26.00	84.65	89.25	1011.98
3500	142.50	52.12	15.68	0.055	102.40	0.87	37.19	26.00	85.06	89.33	1018.64
4000	139.07	58.09	17.90	0.063	117.33	0.87	37.06	26.99	84.89	89.06	1040.69
4500	132.89	62.51	19.94	0.071	132.41	0.87	37.74	27.31	84.77	88.79	1021.50
5000	127.33	66.52	21.89	0.077	147.02	0.87	38.37	27.40	84.74	88.68	1045.68
5500	117.82	67.71	23.11	0.083	160.86	0.88	38.45	27.68	85.07	89.08	1059.05
6000	109.48	68.65	25.12	0.089	173.46	0.86	38.95	27.84	85.15	89.22	1049.35

Table 7: Experimental test results for the engine at different speeds in CNG mode

$n_{es}$ , rpm	$\tau_{et}$ , Nm	$N_e$ , kW	$\dot{m}_f$ , kg/h	$\dot{m}_a$ , kg/s	$\dot{m}_r + \dot{m}_h$ , Lit/min	$\lambda$	$T_{amb}$ , °C	$T_{ain}$ , °C	$T_{win}$ , °C	$T_{wout}$ , °C	$T_{ebc}$ , K
1500	107.99	16.93	4.66	0.018	43.49	0.92	34.30	30.74	84.92	89.17	814.15
2000	110.47	23.07	6.66	0.026	57.91	0.89	33.48	29.47	84.97	88.77	851.15
2500	129.01	33.73	8.62	0.036	72.75	0.96	33.53	29.30	85.11	89.37	921.15
3000	123.71	38.78	10.48	0.042	87.41	0.92	38.80	27.71	84.80	88.68	946.15
3500	119.55	43.73	12.36	0.048	102.31	0.90	38.30	27.53	85.22	89.07	981.15
4000	118.07	49.32	14.05	0.055	117.62	0.90	39.04	27.63	85.11	89.23	1008.15
4500	109.22	51.38	15.60	0.061	132.65	0.91	39.62	27.72	84.97	88.99	1051.15
5000	104.86	54.78	17.17	0.068	147.38	0.91	40.72	27.76	85.17	89.11	1074.15
5500	97.58	56.08	18.25	0.072	161.63	0.91	40.89	28.06	85.29	89.29	1073.15
6000	90.99	57.06	20.04	0.080	174.35	0.92	41.20	28.32	85.01	88.94	1103.15

The defined and measured parameters during the test were almost comprehensive. However, they are presented concisely according to the requirements and purposes of this paper.

### 3. Energy analysis

The energy and entropy balances for an open system under steady state condition are given by Equations (1) and (2) respectively:

Energy balance:

$$\sum_i \dot{m}h - \sum_j \dot{m}h + \sum_s \dot{Q} - \dot{W} = 0 \quad (1)$$

Entropy balance:

$$\sum_i \dot{m}s - \sum_j \dot{m}s + \sum_s \frac{\dot{Q}}{T} + \dot{S}_{gen} = 0 \quad (2)$$

Rate of entropy generation =  $\dot{S}_{gen}$

Fuel energy is given by:

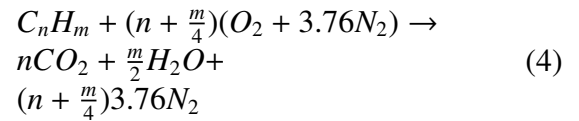
$$\dot{F}_e = \dot{m}_f \cdot LHV \quad (3)$$

Where  $LHV$  and  $\dot{m}_f$  are the lower heating value and the mass flow rate of fuel, respectively.

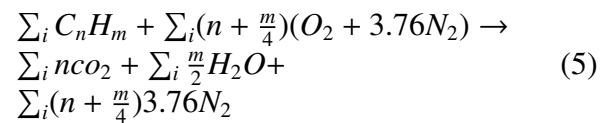
Note that there are some differences in the analysis of energy for both fuels, as the equation of complete combustion and lower heating value of both fuels depend on the chemical composition of the type of fuel. However, the other calculation details are similar.

If one considers the complete combustion of a general hydrocarbon fuel of average molecular composition  $C_nH_m$  with air, the overall complete combustion equation can be written as follows:

Gasoline mode:



CNG is composed of several hydrocarbons with a different weight percentage. Thus, the complete combustion equation can be written as follows:



Therefore, the lower heating value LHV is:

$$LHV_{Gasoline} = n\bar{h}_{f(298K)}^\circ CO_2 + \frac{m}{2}\bar{h}_{f(298K)}^\circ H_2O - \bar{h}_{f(298K)}^\circ C_nH_m \quad (6)$$

$$LHV_{CNG} = \sum_i n\bar{h}_{f(298K)}^\circ CO_2 + \sum_i \frac{m}{2}\bar{h}_{f(298K)}^\circ H_2O - \sum_i \bar{h}_{f(298K)}^\circ C_nH_m \quad (7)$$

Therefore, the lower heating value in gasoline and CNG modes are 42500 (kJ/kg) and 45500 (kJ/kg) respectively.

The power delivered by the engine and absorbed by the dynamometer is the product of torque and angular speed. Note that torque is a measure of an engine's ability to do work whereas power is the rate at which work is done.

In engine tests, the fuel consumption  $\dot{m}_f$  is measured as fuel mass flow per unit time. A more useful parameter is the specific fuel consumption ( $sfc$ ), i.e. the fuel flow rate per unit power output. It measures how efficiently an engine is using the fuel to produce work. Therefore, the specific fuel consumption, ( $sfc$ ) can be estimated.

$$sfc = \frac{\dot{m}_f}{N_e} \quad (8)$$

The following relation gives the overall heat rejection by the cooling water, expressed as a rate of energy flow:

$$\dot{Q}_{cw} = (\dot{m}_r + \dot{m}_h) \left( \frac{C_{p(w)} + C_{p(C_2H_6O_2)}}{2} \right) (T_{wout} - T_{win}) \quad (9)$$

Where:  $\dot{m}_r$ —mass flow rate of radiator,  $\dot{m}_h$ —mass flow rate of heater,  $C_{p(w)}$ —specific heat of water,  $C_{p(C_2H_6O_2)}$ —specific heat of antifreeze (glycol),  $T_{wout}$ —cooling water temperature on engine outlet,  $T_{win}$ —cooling water temperature on engine inlet.

It should be noted that coolant contains 50% water and 50% glycol.

The heat rejection by the exhaust gas is expressed as a rate of energy flow, which is given by Pischinger et al. [16].

$$\dot{Q}_e = (\dot{m}_a + \dot{m}_f)(A + B_1 \cdot T_{ebc} + B_2 \cdot T_{ebc}^2) \quad (10)$$

Where:  $\dot{m}_a$ —mass flow rate of air,  $\dot{m}_f$ —mass flow rate of fuel.

$$A = 8279.49748 - 13744.4871 \cdot \lambda + 5160.91625 \cdot \lambda^2$$

$$B_1 = 1.3509 - 0.59445 \cdot \lambda + 0.2275 \cdot \lambda^2$$

$$B_2 = 0.000154876 - 0.0000752535 \cdot \lambda + 0.000056625 \cdot \lambda^2$$

$T_{ebc}$ —temperature of exhaust manifolds before catalyst,  $\lambda$ —the ratio of mass flow rate fuel/air ( $St$ ) to fuel/air ( $Re$ ).

The miscellaneous heat rejection is expressed as a rate of energy flow given by the following relation:

$$\dot{Q}_{misc} = \dot{F}_e - (N_e + \dot{Q}_e + \dot{Q}_{cw}) \quad (11)$$

Where  $\dot{Q}_{misc}$  is the heat rejection to the oil plus convection and radiation heat transfer from the engine's external surfaces.

Energy efficiency  $\eta_1$  is the ratio of useful output to energy input and is given by the following equation:

$$\eta_1 = \frac{N_e}{\dot{F}_e} \quad (12)$$

#### 4. Exergy analysis

Exergy is composed of two important parts: physical exergy and chemical exergy. In the study, the kinetic and potential parts of exergy are assumed to be negligible. Exergy is defined as the maximum theoretical useful work that can be obtained as a system interacts with an equilibrium state. The chemical exergy is associated with the departure of the chemical composition of a system from its chemical equilibrium. Chemical exergy is an important part of exergy in the combustion process (Ameri et al. [17]).

The following relations give the exergy balances for an open system under steady-state condition:

$$\sum_i \dot{m}e - \sum_j \dot{m}e + \sum_s \dot{Q} \left( 1 - \frac{T_o}{T} \right) - \dot{W} - \dot{E}_d = 0 \quad (13)$$

Rates of exergy transfer =  $\sum_i \dot{m}e - \sum_j \dot{m}e + \sum_s \dot{Q} \left( 1 - \frac{T_o}{T} \right) - \dot{W}$

Rate of exergy destruction =  $\dot{E}_d$

$\dot{Q}$  is the time rate of heat transfer at the boundary of the control volume where the instantaneous temperature is  $T$ .

Finally,  $\dot{E}_d$  accounts for the time rate of exergy destruction owing to irreversibilities within the control volume.

The exergy destruction rate is related to the entropy generation rate.

$$\dot{E}_d = T_o \dot{S}_{gen} \quad (14)$$

Also,  $e$  in Eqn. (13) is the specific exergy, i.e. flow of exergy per unit mass, which consists of  $e_{tm}$  (thermo-mechanical exergy) and  $e_{ch}$  (chemical exergy).

$$e = e_{tm} + e_{ch} \quad (15)$$

Çengel and Boles [18] and Kotas [1] defined thermo-mechanical exergy by the following formula:

$$e_{tm} = h - h_o - T_o(s - s_o) \quad (16)$$

Where  $h$  and  $s$  are the specific enthalpy and entropy of flow at the relevant temperature and pressure, respectively. Also,  $h_o$  and  $s_o$  are the corresponding values of those properties when the flow is at equilibrium conditions with the reference environment.

The specific chemical exergy, for a multi-component stream of the ideal solution, can be estimated using the following relation (Kopac and Kokturk, [9]):

$$\bar{e}_{ch} = \sum_{i=1}^j y_i (\bar{e}_{ch})_i \quad (17)$$

$y_i$  and  $(\bar{e}_{ch})_i$  are the mole fraction of component  $i$  in the mixture and its specific chemical exergy, respectively.

If the component  $i$  exists in the environment, which is also an ideal solution, the specific chemical exergy for each component can be defined as follows:

$$(\bar{e}_{ch})_i = \bar{R}T_o \ln \frac{y_i}{y_i^e} \quad (18)$$

Note that in the analysis of exergy, there is only a difference in the relation of specific chemical exergy of both fuels based on the type of chemical composition.

For the fuel, i.e. a hydrocarbon with the chemical formula  $C_nH_m$ , the following specific chemical exergy can be written (Kopac and Kokturk [9]):

$$\begin{aligned} \bar{e}_{Gasoline}^{C_nH_m} = & \left( \bar{g}_{C_nH_m} + \left(n + \frac{m}{4}\right) \bar{g}_{O_2} - n \bar{g}_{CO_2} - \frac{m}{2} \bar{g}_{H_2O(g)} \right) \\ & + \bar{R}T_o \ln \left[ \frac{(y_{O_2}^e)^{\left(n + \frac{m}{4}\right)}}{(y_{CO_2}^e)^n (y_{H_2O}^e)^{\frac{m}{2}}} \right] \end{aligned} \quad (19)$$

As fuel compositions of CNG are composed of several hydrocarbon with a different weight percentage, the following specific chemical exergy can be written (Kiaahmadi F. [19]):

$$\begin{aligned} \bar{e}_{CNG}^{C_nH_m} = & \left( \sum_i \bar{g}_{C_nH_m} + \sum_i \left(n + \frac{m}{4}\right) \bar{g}_{O_2} - \sum_i n \bar{g}_{CO_2} - \sum_i \frac{m}{2} \bar{g}_{H_2O(g)} \right) \\ & + \bar{R}T_o \ln \left[ \frac{(y_{O_2}^e)^{\sum_i \left(n + \frac{m}{4}\right)}}{(y_{CO_2}^e)^{\sum_i n} (y_{H_2O}^e)^{\sum_i \frac{m}{2}}} \right] \end{aligned} \quad (20)$$

The chemical exergy for the fuel is estimated by assumption of a chemical reaction where it reacts with the oxygen and is completely changed into products which exist in the environment.

The exhaust exergy  $\dot{E}_e$  is the sum of the thermo-mechanical and the chemical exergy of each component and is calculated by Equations (15) to (20) using the calculated exhaust gas compositions.

Heat exergy,  $\dot{E}_Q$ , is given by the following relation:

$$\dot{E}_Q = \left(1 - \frac{T_o}{T}\right) \dot{Q} \quad (21)$$

Work exergy,  $\dot{E}_w$ , is given by the following relation:

$$\dot{E}_w = \dot{W} = N_e \quad (22)$$

Fuel exergy,  $\dot{E}_f$ , is given by the following relation:

$$\dot{E}_f = \dot{m}_f \cdot e_{ch,f} \quad (23)$$

Exergy efficiency  $\eta_{II}$ , can be calculated by the following relation:

$$\eta_{II} = \frac{\text{Exergy recovered}}{\text{Exergy supplied}} = \frac{\dot{E}_R}{\dot{E}_s} = 1 - \frac{\text{Exergy destroyed}}{\text{Exergy supplied}} = 1 - \frac{\dot{E}_d}{\dot{E}_s} \quad (24)$$

The supplied exergy  $\dot{E}_s$  and the recovered exergy  $\dot{E}_R$ , are given by the following relations:

$$\dot{E}_s = \dot{E}_f - \dot{E}_e - \dot{E}_Q, \dot{E}_R = \dot{E}_w \quad (25)$$

## 5. Results and discussion

The experimental data, which are given in Tables 6 and 7, are used to perform the energy and exergy analysis of the engine for different speeds. Table 8 shows the energy balance breakdown (%) at full load state for different speeds in gasoline and CNG modes. The results show that, using gasoline and CNG fuel, the heat rejection of energy flow increases with increasing engine speed owing to the increased fuel energy entering the engine. The heat rejection from the engine can be reduced by insulating the

Table 8: Energy balance breakdown (%) at full load state for different speeds in gasoline and CNG modes

$n_{es}$ , rpm	at gasoline mode					at CNG mode				
	$\dot{F}_e$ , %	$\eta_1$ , %	$\dot{Q}_{cw}$ , %	$\dot{Q}_e$ , %	$\dot{Q}_{misc}$ , %	$\dot{F}_e$ , %	$\eta_1$ , %	$\dot{Q}_{cw}$ , %	$\dot{Q}_e$ , %	$\dot{Q}_{misc}$ , %
1500	100	28.38	16.76	25.31	29.54	100	28.73	17.03	31.05	23.19
2000	100	26.97	14.06	41.50	17.46	100	27.39	14.17	36.05	22.39
2500	100	30.42	15.39	37.84	16.35	100	30.97	15.46	30.46	23.11
3000	100	29.66	14.08	40.95	15.31	100	29.28	13.89	35.95	20.88
3500	100	28.16	12.82	45.56	13.46	100	27.98	13.68	39.32	19.02
4000	100	27.49	12.56	46.29	13.66	100	27.77	14.80	40.78	16.65
4500	100	26.56	12.26	45.42	15.76	100	26.06	14.69	41.73	17.52
5000	100	25.74	12.14	46.78	15.35	100	25.24	14.49	42.49	17.77
5500	100	24.82	12.81	45.83	16.55	100	24.32	15.21	42.77	17.70
6000	100	23.15	12.89	46.96	17.00	100	22.53	14.67	42.69	20.11

walls of the combustion chamber. However, it will cause an increase in the temperature of the exhaust gas, thus increasing the energy loss due to the exhaust gas. This energy loss is really the difference between the fuel energy input and the sum of heat rejection of energy flow and useful work transfers from the control volume. The exhaust loss is only a function of the difference between the fuel energy input and the heat rejection of energy flow rate from the control volume. The energy that is lost by hot gases increases as the speed increases. The energy, which is lost by the cooling system, is higher at low speeds and decreases as the speed increases. The possibility of extracting energy from the cooling water is almost remote, as it has a low temperature. The results show that the exhaust gas heat rejection has the maximum share in the energy balance for all speeds, as it has the highest heat value.

The ratio of heat rejection by the exhaust gas increases with a decrease in the ratio of the fuel mass flow rate to the air mass flow rate for the combustion process. The results show that 17.04% in gasoline mode and 19.83% in CNG mode of the fuel energy input, on average, is lost due to the miscellaneous heat rejection from the engine. This energy loss is the heat rejected to the oil plus convection and radiation from the engine's external surfaces. The results show that for both gasoline and CNG fuels, the maximum efficiency of engine occurs at approximately 2500 rpm, and the efficiency decreases as the speed

increases. In addition, the energy, which is lost by the cooling system, is higher at low speeds and decreases as the speed increases. In contrast, the energy that is lost by hot gases increases as the speed increases.

However, it can be mentioned that the change in fuel type for the engines that are designed to use gasoline-fuel, could increase the temperature of the engine. Nevertheless, the results in Tables 6 and 7 show that at full load state the surface temperature of the combustion compartment and the temperature of output gases for CNG-fuel engines are lower than with the gasoline-fuel engines. These temperatures are very sensitive to the fuel air ratio and the advance angle of the spark. Therefore, this increase in temperature for practical application of the engine on the road is due to changes in these parameters. In fact, it is not essentially due to a change of the fuel type from gasoline to natural gas (Raine and Jones, [20]).

Table 9 show the exergy balance breakdown (%) for different speeds in gasoline and CNG modes. The results show that for gasoline and CNG fuels the heat rejection exergy rises as engine speed increases, which is due to the increased fuel exergy entering the engine. In addition, it is clear that the exergy destroyed in combustion has the maximum magnitude for various speeds. The minimum exergy destroyed in combustion occurs at maximum exergy efficiency. A significant fraction of the fuel exergy is destroyed by irreversible processes in the engine, such as combustion, heat transfer, friction, etc. The ratio of ex-

Table 9: Exergy balance breakdown (%) for different speeds in gasoline and CNG modes

$n_{es}$ , rpm	at gasoline mode						at CNG mode					
	$\dot{E}_f$ , %	$\eta_{II}$ , %	$\dot{E}_w$ , %	$\dot{E}_e$ , %	$\dot{E}_Q$ , %	$\dot{E}_d$ , %	$\dot{E}_f$ , %	$\eta_{II}$ , %	$\dot{E}_w$ , %	$\dot{E}_e$ , %	$\dot{E}_Q$ , %	$\dot{E}_d$ , %
1500	100	30.17	26.42	9.41	3.03	61.14	100	30.74	27.01	8.89	3.24	60.86
2000	100	28.64	25.10	10.10	2.25	62.55	100	29.42	25.75	9.93	2.52	61.80
2500	100	33.42	28.31	13.30	1.98	56.41	100	33.72	29.12	10.93	2.74	57.22
3000	100	34.00	27.61	14.41	4.38	53.60	100	34.08	27.52	13.63	5.61	53.24
3500	100	32.05	26.21	14.44	3.77	55.58	100	32.41	26.31	13.78	5.03	54.88
4000	100	31.43	25.59	15.13	3.45	55.83	100	32.32	26.11	14.62	4.57	54.69
4500	100	30.36	24.72	14.53	4.06	56.69	100	31.00	24.50	16.02	4.95	54.53
5000	100	29.71	23.96	15.29	4.08	56.67	100	30.46	23.73	16.77	5.32	54.18
5500	100	28.88	23.10	15.71	4.31	56.88	100	29.29	22.86	16.74	5.22	55.18
6000	100	26.90	21.54	15.40	4.51	58.54	100	27.74	21.18	17.72	5.91	55.19

exergy destruction decreases as the mass of air to the mass of fuel ratio increases for a combustion process. Other sources of irreversibility or destruction of exergy such as friction and heat transfer also tend to rise as engine speed increases. The reduction in exergy destruction is due to the fact that the exergy content of the exhaust heat also increases with engine speed. The use of exhaust recovery devices such as a supercharger system are recommended to utilize the exergy of hot exhaust gases. There are three exergy losses from the control surface. They are exergy losses due to heat transfer, mass transfer and work. The results show that almost 2% to 4.5% of the fuel exergy input is exergy loss due to heat transfer from the engine in gasoline mode. Moreover, 9.4% to 15.7% of the fuel exergy input is exergy loss due to mass transfer of the exhaust gas flow from the engine. This loss can be decreased by reducing the exhaust gas temperature. However, in CNG mode, almost 2.52 to 5.91% of the fuel exergy input is exergy loss due to heat transfer from the engine. On the other hand, 8.9% to 17.7% of the fuel exergy input is exergy loss due to the mass transfer of exhaust gas flow from the engine. This loss can be decreased by reducing the exhaust gas temperature as well.

Tables 8 to 9 indicate that the energy and exergy efficiencies, for both gasoline and CNG fuels, have maximum points at 2500 rpm and 3000 rpm respectively.

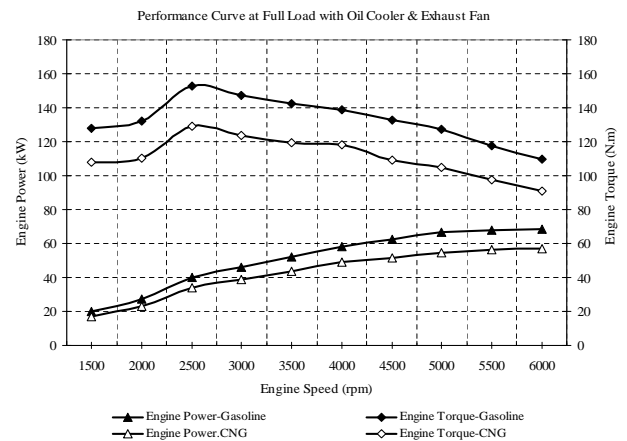


Figure 2: Engine power and Engine torque of gasoline and CNG vs. engine speed

The results show that the fuel exergy inputs are 6.93% higher than the corresponding fuel energy inputs for gasoline mode. Also, the fuel exergy inputs are 5.98% higher than the corresponding fuel energy inputs for CNG mode. Figure 2 demonstrates the power and torque of the gasoline and CNG curve versus the engine speed. It shows that, using gasoline and CNG fuel, engine power increases with speed. However, the torque increases to a maximum point at 2500 rpm and decreases after this point because of volumetric efficiency drop. The maximum engine power for both fuels occurs at the maximum speed, i.e. 6000 rpm. However, the maximum power for

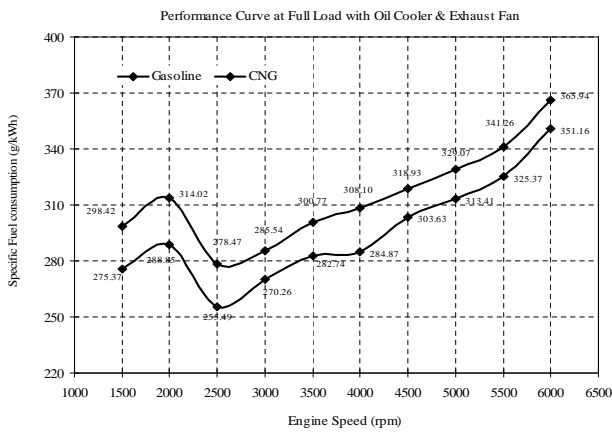


Figure 3: Specific fuel consumption of gasoline and CNG vs. engine speed

CNG is 20.3% less than the maximum power for gasoline. Also, the maximum torque for CNG is 18.4% less than the corresponding value for gasoline. The results show that due to volumetric efficiency drop, the power and torque of the CNG-fuel engine is lower than gasoline-fuel one. Due to the simple and dense structure of the methane molecule (which has the maximum amount in natural gas composition), natural gas is extremely resistant to knocking. Engines that use natural gas can obtain higher compression ratios and efficiencies due to the high octane number and zero sensitivity coefficient. However, as gasoline-fuel engines operate at lower compression ratios, they cannot achieve high efficiencies, in contrast to natural gas fuel-engines. Therefore, it is recommended to use a turbocharger system to compensate for the decrease in power and torque of the natural gas fuel-engines without running the risk of knocking.

Figure 3 shows the specific fuel consumption of gasoline and CNG versus engine speed. The specific fuel consumption reduces to a minimum at 2500 rpm, which is exactly the same speed for the maximum torque point. The curves show that the specific fuel consumption at full load condition and low speed (2000 rpm) is high. The specific fuel consumption increases as the speed increases. Nevertheless, it should be emphasized that the specific fuel consumption increases from 1500 rpm to 2000 rpm and decreases up to 2500 rpm. These changes are related to the  $\lambda$  measured at different engine speeds

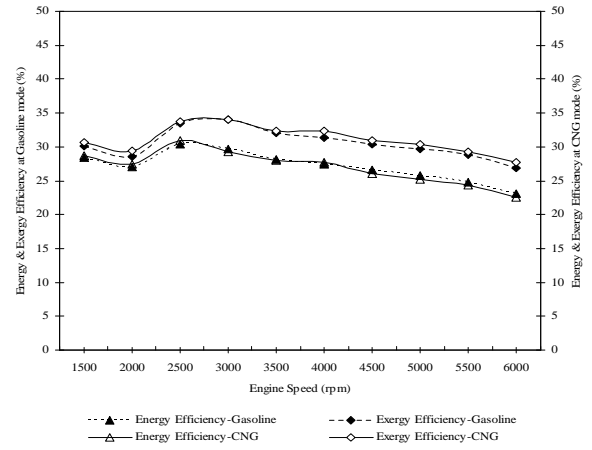


Figure 4: Energy efficiency and exergy efficiency of gasoline and CNG vs. engine speed

(Tables 6 and 7). For two different engine speeds, namely 2500 rpm and 3000 rpm, specific fuel consumptions at gasoline and CNG modes are (278.47, 285.54 g/(kW·h)) and (255.49, 270.26 g/(kW·h)) respectively. In fact, energy efficiency as a function of engine speed can be deduced from the specific fuel consumption as a function of engine speed; where the former exhibits a maximum, the latter goes through a minimum. As far as the energy analysis is concerned, there is no significant difference between 2500 and 3000 rpm as the optimum speed. Nevertheless, the exergy analysis at gasoline and CNG modes (Table 9) clearly indicates that 3000 rpm is the optimum speed since it is associated with higher exergy efficiency. The results show that the specific fuel consumption of the CNG fuel engine is lower than that of the gasoline-fuel engine. In fact due to the characteristics of natural gas, it occupies the whole capacity of input manifold volume. Therefore, the mass flow rate of the input air to engine decreases. Alternatively, as the capacity of the input manifold is invariable, the mass flow of the input fuel is less and consequently, specific fuel consumption of the engine decreases.

The results show that the exergy curve trend is similar to the energy balance curve for gasoline and CNG fuels. However, the only difference is the fact that maximum exergy efficiency occurs at a speed that is marginally higher than the maximum energy efficiency speed, as explained earlier. This fact is clearly shown in Figure 4 as well. It shows that en-

ergy efficiency has a maximum point at the speed of 2500 rpm whereas exergy efficiency has a maximum at a speed of 3000 rpm. Moreover, it is clear that exergy efficiency, in contrast to energy efficiency, gives us better results as well. Exergy efficiency has a maximum point where the exergy destruction of combustion reaches its minimum. Exergy efficiencies in gasoline mode (5.83–14.05%) and at CNG mode (6.53–18.78%) are higher than the corresponding energy efficiencies, because a higher amount of fuel exergy compared to fuel energy, is supplied to the engine. Since exergy efficiency takes into account both the first and the second law of thermodynamics, it provides a better measure of performance for a thermal system. Therefore, one can conclude that the exergy analysis reveals that the engine optimum speed is 3000 rpm, as exergy efficiency has maximum magnitude at this speed. Moreover, exergy efficiency for the CNG-fuel engine is higher than for the gasoline-fuel engine for all speeds. This could be due to the magnitude of the natural gas octane number. In fact, natural gas has better efficiency compared to gasoline owing to its endurance at higher octane numbers. For all conditions, natural gas has more exergy than gasoline. However, liquid fuels like gasoline have many important advantages like much greater volumetric energy density, ease of transport and storage, which have made them the fuels of choice for IC engines.

## 6. Conclusions

This study presents both experimental measurements and an analytical assessment of a dual-fuel internal combustion engine based on energy and exergy analysis.

On the basis of those analyses, one can draw the following conclusions:

- The results show that due to volumetric efficiency drop, the power and torque of the CNG-fuel engine is lower than for the gasoline-fuel engine.
- The specific fuel consumption for both fuels reduces to a minimum at 2500 rpm, which is exactly the same speed for the maximum torque point. The results show that the specific fuel consumption of the gasoline-fuel engine is higher than the CNG-fuel engine.
- The results show that the energy and exergy of the heat rejection for gasoline and CNG fuels rise with increasing engine speed and the energy efficiencies are slightly lower than the corresponding exergy efficiencies.
- The energy that is lost by hot gases for both fuels rises as the speed increases. The energy, which is lost by the cooling system, is higher at low speeds and decreases as the speed increases.
- The ratio of the heat rejection by the exhaust gas increases with a decrease in the fuel to the air mass flow rate ratio for a combustion process. The results show that, on average, 17.04% in gasoline mode and 19.83% in CNG mode, of the fuel energy input is lost due to miscellaneous heat rejection from the engine.
- The energy and exergy efficiencies, for both gasoline and CNG fuels, have maximum points at the speed of 2500 rpm and 3000 rpm respectively. The results show that the fuel exergy inputs are 6.93% higher than the corresponding fuel energy inputs for gasoline mode. Also, the fuel exergy inputs are 5.98% higher than the corresponding fuel energy inputs for CNG mode.
- The exergy analysis in gasoline and CNG modes clearly indicates that 3000 rpm is the optimum speed, since it is associated with higher exergy efficiency.
- The exergy efficiency for the CNG-fuel engine is higher than gasoline-fuel engine exergy efficiency for all speeds. This could be caused by the magnitude of the natural gas octane number.
- Irreversible processes in the engine, such as combustion, heat transfer and friction, destroy a significant fraction of the fuel exergy. Moreover, sources of exergy destruction such as friction and heat transfer also tend to increase with an increase in engine speed.

The results show that the use of a combined energy and exergy analysis provides better criteria for the performance assessment of a thermal system.

### Acknowledgments

The authors would like to thank the Iran Khodro Powertrain Company (IPCO) for supporting this research and providing the engine experimental set up.

### References

- [1] T. Kotas, The Exergy Method of Thermal Plant Analysis, Butterworths, London, 1985.
- [2] I. Dincer, The role of exergy in energy policy making, Energy Policy 30 (2) (2002) 137–149.
- [3] F. N. Alasfour, Butanol—a single-cylinder engine study: availability analysis, Applied Thermal Engineering 17 (1997) 537–549. doi:10.1016/S1359-4311(96)00069-5.
- [4] A. C. Alkidas, The application of availability and energy balances to a diesel engine, Journal of Engineering for Gas Turbines and Power 110 (3) (1988) 462–469. doi:10.1115/1.3240143.  
URL <http://link.aip.org/link/?GTP/110/462/1>
- [5] W. Lipkea, A. DeJooode, A comparison of the performance of two direct injection diesel engines from a second law perspective, in: SAE Paper, no. 890824, 1998.
- [6] J. Caton, A review of investigations using the second law of thermodynamics to study internal combustion engines, in: SAE Paper, 2000.
- [7] C. Rakopoulos, E. Giakoumis, Second law analyses applied to internal combustion engines operation, Progress in Energy and Combustion Science 32 (2006) 2–47.
- [8] J. A. Caton, On the destruction of availability (exergy) due to combustion processes – with specific application to internal-combustion engines, Energy 25 (11) (2000) 1097 – 1117. doi:10.1016/S0360-5442(00)00034-7.
- [9] M. Kopac, L. Kokturk, Determination of optimum speed of an internal combustion engine by exergy analysis, International Journal of Exergy 2 (1) (2005) 40–54.
- [10] C. Rakopoulos, D. Kyritsis, Comparative second-law analysis of internal combustion engine operation for methane, methanol, and dodecane fuels, Energy 26 (7) (2001) 705 – 722. doi:10.1016/S0360-5442(01)00027-5.
- [11] C. Sayin, M. Hosoz, M. Canakci, I. Kilicaslan, Energy and exergy analyses of a gasoline engine, International Journal of Energy Research 31 (3) (2007) 259–273. doi:10.1002/er.1246.  
URL <http://dx.doi.org/10.1002/er.1246>
- [12] K. Nakonieczny, Entropy generation in a diesel engine turbocharging system, Energy 27 (2002) 1027–1056.
- [13] C. Rakopoulos, E. Giakoumis, Availability analysis of a turbocharged diesel engine operating under transient load conditions, Energy 29 (8) (2004) 1085–1104.
- [14] M. Canakci, M. Hosoz, Energy and exergy analyses of a diesel engine fuelled with various biodiesels, Energy Sources 1 (2006) 379–394.
- [15] M. Ameri, F. Kiaahmadi, M. Khanaki, M. Nazoktabar, Energy and exergy analyses of a spark-ignition engine, International Journal of Exergy 7 (5) (2010) 547–563. doi:10.1504/IJEX.2010.034928.
- [16] R. Pischinger, G. Krassnig, G. Taucar, T. Sams, A. Pischinger, Die Thermodynamik der Verbrennungskraftmaschine, Neue Folge B and 5. Von List H, 10/1998.
- [17] M. Ameri, P. Ahmadi, S. Khanmohammadi, Exergy analysis of a 420 mw combined cycle power plant, International Journal of Energy Research 32 (2008) 175–183.
- [18] A. Cengel, M. Boles, Thermodynamics, An Engineering Approach, McGraw-Hill, New York, 1998.
- [19] F. Kiaahmadi, The performance evaluation of an internal combustion engine by exergy analysis, Master's thesis, PWUT (2008).
- [20] R. Raine, G. Jones, Comparison of temperatures measured in natural gas and gasoline fuelled engines, in: SAE paper, no. 901503, Department of mechanical engineering, University of Auckland, 1990.

### Nomenclature

- $n_{es}$ —engine speed, rpm  
 $\tau_{et}$ —engine torque, Nm  
 $N_e$ —engine power, kW  
 $\dot{m}_f$ —mass flow rate of fuel, kg/h  
 $\dot{m}_r$ —mass flow rate of radiator, Lit/min  
 $\dot{m}_h$ —mass flow rate of heater, Lit/min  
 $\dot{m}_a$ —mass flow rate of air, kg/s  
 $T_{wout}$ —Cooling water temperature at engine outlet, °C  
 $T_{win}$ —cooling water temperature at engine inlet, °C  
 $T_{ebc}$ —temperature of exhaust gas before entry into the catalyst, °C  
 $T_{ain}$ —air temperature at engine intake, °C  
 $T_{amb}$ , Ambient air temperature, °C  
 $\lambda$ —ratio mass flow rate fuel/air (St) to fuel/air (Re)  
 $LHV$ —lower heating value (kJ kg<sup>-1</sup>)  
 $sfc$ —specific fuel consumption, g/(kW·h)  
 $C_{p(w)}$ —specific heat of water, kJ/(kg·K)  
 $C_{p(C_2H_6O_2)}$ —specific heat of antifreeze (glycol), kJ/(kg·K)  
 $\dot{Q}$ —heat transfer, kW  
 $\dot{Q}_e$ —exhaust gas heat rejection, kW  
 $\dot{F}_e$ —fuel energy, kW  
 $\dot{Q}_{cw}$ —cooling water heat rejection, kW  
 $\dot{Q}_{misc}$ —miscellaneous heat rejection, kW

$e$ —total exergy, kJ/kg  
 $e_{ch}$ —chemical exergy, kJ/kg  
 $\bar{e}_{ch}$ —chemical exergy, kJ/kmol  
 $e_{tm}$ —thermo-mechanical exergy, kJ/kg  
 $\dot{E}_d$ —exergy destroyed, kW  
 $\dot{E}_e$ —exhaust exergy, kW  
 $\dot{E}_S$ —exergy supplied, kW  
 $\dot{E}_f$ —fuel exergy, kW  
 $\dot{E}_w$ —work exergy, kW  
 $\bar{g}$ —Gibbs free energy, kJ/kmol  
 $h$ —enthalpy, kJ/kg  
 $h_o$ —enthalpy at environmental condition, kJ/kg  
 $P$ —pressure, kPa  
 $P_o$ —environmental pressure, kPa  
 $R$ —universal gas coefficient, kJ/(kmol·K)  
 $s$ —entropy, kJ/(kg·K)  
 $s_o$ —entropy at environmental condition, kJ/(kg·K)  
 $\dot{S}_{gen}$ —entropy generation in the system, kW/K  
 $T$ —temperature, K  
 $T_o$ —environmental temperature, K  
 $\dot{W}$ —work of control volume, kW  
 $y_i$ —mole fraction of component  $i$  in the exhaust gas  
 $y_i^e$ —mole fraction of component  $i$  in the environment  
 Greek symbols  
 $\eta_1$ —energy efficiency  
 $\eta_{II}$ —exergy efficiency